

Scintillation Effects on Radio Wave Propagation Through Solar Corona

C. M. Ho, M.K. Sue, A. Bedrossian, and R. W. Sniffin

Jet Propulsion Laboratory, California Institute of Technology,
Pasadena, CA 91109, USA

Abstract: When RF waves pass through the solar corona and solar wind regions close to the Sun, strong scintillation effects appear at their amplitude, frequency and phase, especially in the regions very close to the Sun (less than 4 solar radius). After analyzing recent solar corona conjunction experimental data at S, X and Ka bands, we have developed a group of empirical equations to describe these effects on telecommunication links over microwave frequency ranges. There are mainly three types of degradation effects on RF signals: (1) Intensity scintillation (rapid signal amplitude changes due to propagation path changes and phase shifting scattered by corona turbulence) (2) Phase scintillation (signal frequency fluctuations due to rapid phase changes through solar corona turbulence) (3) Spectral broadening (Doppler shifting of RF signals scattered by moving plasma irregularities). We find that all of three degradation quantities may be represented in a simplified form: $\alpha f^\beta RTEC^\gamma$ where α , β and γ are three constants with different values for different quantities, f is RF signal frequency, while $RTEC$ (radial total electron contents) is an integration of plasma density along the radial direction starting from the ray path's closest distance from the Sun to infinity. In this study, all constants for above equation are determined through the data fitting and the RF signal frequency dependence for all solar corona effects are summarized.

1. Introduction: The solar corona and solar wind are high density and strongly turbulent ionized gases erupted from the Sun in comparison with the Earth's ionosphere. When RF waves pass through the ionized gas regions as shown in Figure 1, the signals cause strong scintillation at their amplitude, frequency and phase, especially in the regions very close to the Sun (less than 4 solar radius). These effects will severely degrade the telecommunication links and even make it impossible [1,2,3,4]. Recent solar corona conjunction experiments for the first time made it available to detect these scintillation effects at S, X and Ka bands [5,6,7,8,9]. This study briefly summarizes the primary effects of the solar corona and solar wind on telecommunications parameters as related to the DSN (Deep Space Network) at S (2.3 GHz), X (8.4 GHz) and Ka (32 GHz) band radio signals passing through the solar corona and solar wind. It allows the telecommunications engineer to predict radio metric and radio science data performance of signals.

2. Effects in Solar Corona: Because of much strong turbulence and irregularities, solar corona and near-Sun solar wind are an inhomogeneous plasma medium, especially, within 4 solar radius. In addition to the effects in homogeneous plasma (such as group delay, dispersion, Faraday rotation, absorption and phase advance, etc.), radio signals will suffer the following significant degradation:

2.1. Intensity Scintillation [1,9]: RF signals passing through solar corona will be scattered by turbulence. Rapid amplitude changes around their average will occur due to each wave ray path changes and phase shifting. Thus, instantaneous SNR degradation occurs. The intensity scintillation can be described using an index, m , which is defined as the rms signal intensity fluctuation relative to the mean intensity. It characterizes the strength of small-scale charged particle density fluctuations for a weak scintillation. Because scintillations are strongly related to the plasma density at the closest distance from the Sun [1,9], it is found that the index can be expressed using a simplified empirical equation as:

$$m = a_0 f^{-1.42} RTEC \quad (m \leq 1) \quad (1)$$

where $a_0 = 2.07 \times 10^{-20}$; f is signal frequency in GHz, and $RTEC$ (radial total electron contents) is defined as an integration along the radial direction starting from a , the ray path's closest distance from the Sun, to infinity:

$$RTEC = d_0 \int_a^\infty N_e(r) dr \quad (2)$$

where d_0 is a constant ($d_0 = 5.9$) and N_e is solar wind electron density, a function only of radial distance r . At low heliospheric latitude and equatorial regions, it can be approximately modeled as [10]:

$$N_e(r) = 2.21 \times 10^{14} \left(\frac{r}{R_o}\right)^{-6} + 1.55 \times 10^{12} \left(\frac{r}{R_o}\right)^{-2.3} \quad (3)$$

where R_o is solar radius (6.97×10^8 m), r in meter and $N_e(r)$ in m^{-3} . As a comparison, we have also define a slant total electron contents ($STEC$) as $STEC = \int_L N_e dl$, an integration along the entire propagation path L from Earth station to spacecraft [11]. Note that this integration is a function of angles α and β which uniquely define the path L (see Figure 1).

Using Equations (2) and (3), we have

$$RTEC = 1.82 \times 10^{23} \left(\frac{a}{R_o}\right)^{-5} + 4.29 \times 10^{21} \left(\frac{a}{R_o}\right)^{-1.3} \quad (4)$$

When $a = 4 R_o$, $RTEC = 9.86 \times 10^{20} m^{-2}$. The integrated $RTEC$ for various R_o and $STEC$ values for various α and β are shown in Figure 2. The former integration has a much simpler analytical solution than the latter does. SNR and intensity scintillation index from first Cassini solar conjunction for both X and Ka bands are shown in Figures 3a, 3b, 3e and 3f, respectively. Figure 4 shows the indices m verse SEP (sun-earth-probe angle) and the fit using previous data.

2.2. Phase Scintillation [1,9]: Frequency fluctuations will occur due to the rapid phase changes of the signals passing through the solar corona turbulence. Phase scintillation is a type of Doppler noise after excluding the frequency changes due to spacecraft motion. The Doppler noise (or phase scintillation) is defined as σ_D (Hz), the rms frequency residuals in which a trend is removed, as shown in Figure 3c (for X band) and 3d (for Ka band). It is found that σ_D can also be expressed using a simplified empirical equation as:

$$\sigma_D = b_0 f^{-1} RTEC \quad (5)$$

where $b_0 = 1.64 \times 10^{-21}$, f is signal frequency in GHz, and $RTEC$ is defined in (4). Figure 5 shows σ_D measurements at S band and curves from equation (5) for three frequency bands.

2.3. Spectral Broadening [1,9]: Spectral broadening arises because of Doppler shifting of the radio signal as it is scattered by moving plasma irregularities. Its bandwidth, B , is defined as half of the signal power located. Figure 6 shows examples of spectral broadening with decreasing distance from the Sun. An empirical formula for spectral broadening bandwidth is:

$$B = c_0 f^{-1.2} RTEC^{1.2} \quad (6)$$

where $c_0 = 1.14 \times 10^{-24}$, f is signal frequency in GHz, and $RTEC$ is defined in (4). There is a relation between spectral broadening bandwidth B and phase scintillation Doppler noise σ_D :

$$B = 10.0 \sigma_D^{1.2} \quad (7)$$

Figure 7 shows Cassini measurements for X and Ka bands and curves based on an extrapolated model. Figure 8 shows spectral broadening measurements and curves from equation (6) for three frequency bands.

3. Effects on Frequency Dependence: The frequency dependence for all solar wind effects is summarized in Table 1. Typical values for a 2.3 GHz radio ray path with a $4 R_s$ closest distance from Sun are given. All of the effects are reduced as radio signal frequency increases. The solar cycle dependence for all the effects is not obvious. At a region near the sun, all scintillation effects are strongly related to solar wind turbulence.

4. Summary: We have described the impact of the solar corona and solar wind on telecommunications when radio wave ray path has a closest distance less than 10 solar radius from the center of Sun. After analyzing recent solar corona conjunction experimental data at S-, X- and Ka-bands, we have developed a group of empirical equations to describe these degradation effects on telecommunication links over microwave frequency ranges. Three degradation quantities (intensity scintillation, phase scintillation and spectral broadening) for RF signals may be represented in a simplified form: $\alpha f^\beta RTEC^\gamma$ where α , β , and γ are three constants with different values for different quantities, f is RF signal frequency, while $RTEC$ (radial total electron contents) is an integration of plasma density along the radial direction starting from the ray path's closest distance from the Sun to infinity. All constants for above equation have been determined through the data fitting. The RF signal frequency dependence for all solar corona effects are also summarized in a table.

Table 1. Solar Corona Effect Dependence on Signal Frequency

Effects	Typical Value (at 2.3 GHz, 4 R_{\odot})	Frequency Dependence (f)
Group Delay	17 μ sec (250 nsec in ionosphere)	$1/f^2$
Dispersion	10 nsec/MHz	$1/f^3$
Absorption	negligible	$1/f^2$
Faraday Rotation	20°-200° (3°-7° in ionosphere)	$1/f^2$
Phase Advance	1.07×10^5 rad	$1/f^4$
Intensity Scintillation	Saturates at $m = 1$	$1/f^{d.42}$ to $1/f^{d.2}$
Phase Scintillation	< 1 Hz	$1/f^d$
Spectral Broadening	~ 10 Hz	$1/f^{d.2}$ to $1/f^d$
Angular Broadening	0.02 – 2 min arc	$1/f^{d.2}$ to $1/f^d$

References

- [1] Woo, R., Measurements of the solar wind using spacecraft radio scattering observations, *Study of Travelling Interplanetary Phenomena*, eds. By M.A.Shea et al., Reidel Publishing Company, Dordrecht-Holland, 1977.
- [2] Armstrong, J. W., and Woo, R., Solar wind motion within 30 R_{\odot} : Spacecraft radio scintillation observations, *Astronomy and Astrophysics*, 103, 415, 1981.
- [3] Woo, R. and Armstrong, J. W., Observations of large-scale structure in the inner heliosphere with doppler scintillation measurements, *Solar Wind*, eds. E. Marsch and R. Schwenn, Pergamon Press, Oxford, 319-322, 1992.
- [4] Fera, Y., et al., Solar scintillation effects on telecommunication links at Ka-band and X-band, *TDA Progress Report 42-129*, Jet Propulsion Laboratory, Pasadena, California, 1997.
- [5] Morabito, D., et al., The Mars Global Surveyor Ka-band link experiment (MGS/KaBLE-II), *TDA Progress Report 42-137*, Jet Propulsion Laboratory, Pasadena, California, May 15, 1999.
- [6] Bokulic, R.S., and W. V. Moore, Near Earth Asteroid Rendezvous (NEAR) spacecraft solar conjunction experiment, *Journal of Spacecraft and Rockets*, 36, 87, 1999.
- [7] Morabito, D., et al., The 1998 Mars Global Surveyor solar corona experiment, *TMO Progress Report 42-142*, Jet Propulsion Laboratory, Pasadena, California, August 15, 2000.
- [8] Morabito, D., and R. Hastrup, Communications with Mars during periods of solar conjunction: Initial study results, *IPN Progress report*, 42-147, Jet Propulsion Laboratory, Pasadena, California, Nov. 2001.
- [9] Morabito, D., et al., The Cassini May 2000 solar conjunction, to appear in *IEEE Transactions on Antenna and Propagation*, 2002.
- [10] Berman, A.L., A unified observational theory for solar wind columnar turbulence, *DSN Progress report 42-50*, p743, Jet Propulsion Laboratory, Pasadena, California, 1979.
- [11] Berman, A.L., and J.A. Wackley, Doppler noise considered as a function of the signal path integration of electron density, *DSN Progress Report 42-33*, p159, Jet Propulsion Laboratory, Pasadena, California, 1976.

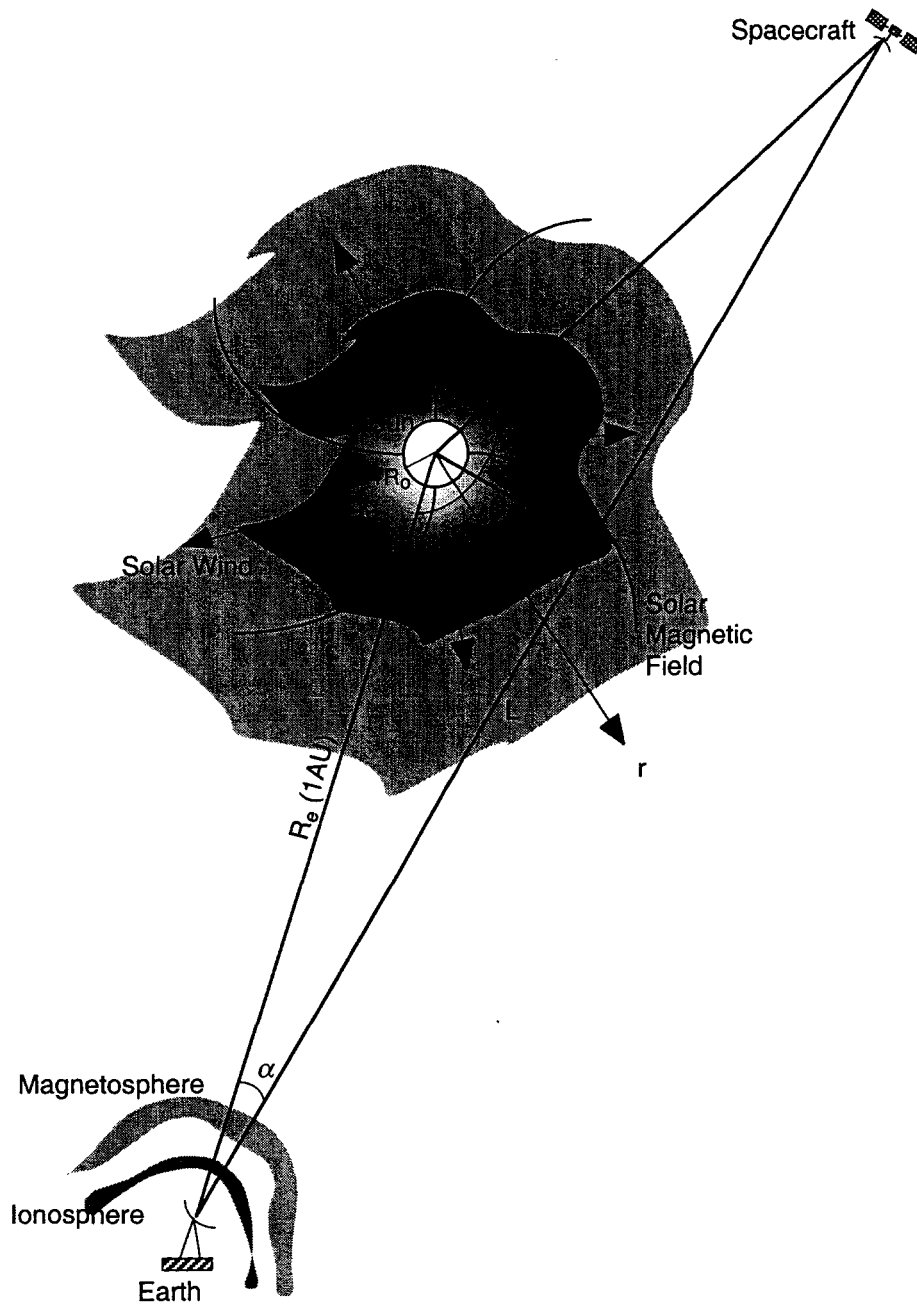


Figure 1. A geometric diagram showing the radio wave ray from spacecraft passing through the solar corona near the solar conjunction and received by the earth station. The shaded areas show inhomogeneous solar corona plasma regions with high density. The path has a closest distance from the sun as a . Sun-earth-spacecraft angle or elongation angle is α (1 solar radius in $a = 0.25^\circ$ in α). Spacecraft-Sun-Earth angle is β and signal path length is L between spacecraft and earth station. Solar wind plasma density decreases with radial distance while solar magnetic field has a spiral shape. Around Earth station, the ionosphere and magnetosphere with relatively low plasma density are also shown.

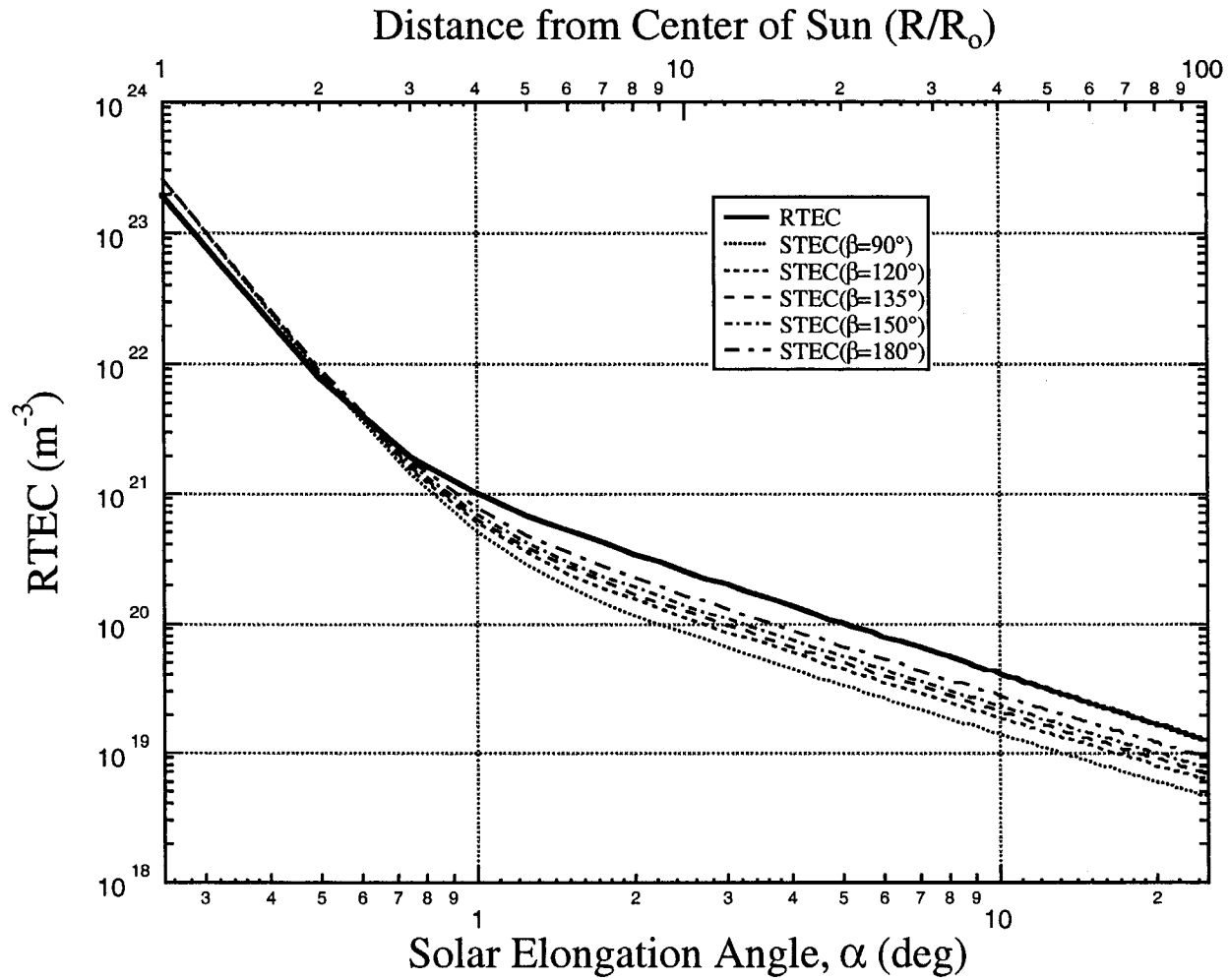


Figure 2. A comparison of the radial total electron contents (*RTEC*) from the closest solar radial distance R_0 with the slant total electron contents (*STEC*) along a propagation path L . Here, $STEC = \int_l N_e dl$ is an integration of solar wind electrons along the entire path L from earth station to spacecraft. The integration is a function of both angles α and β which uniquely define the path L (see Figure 1).

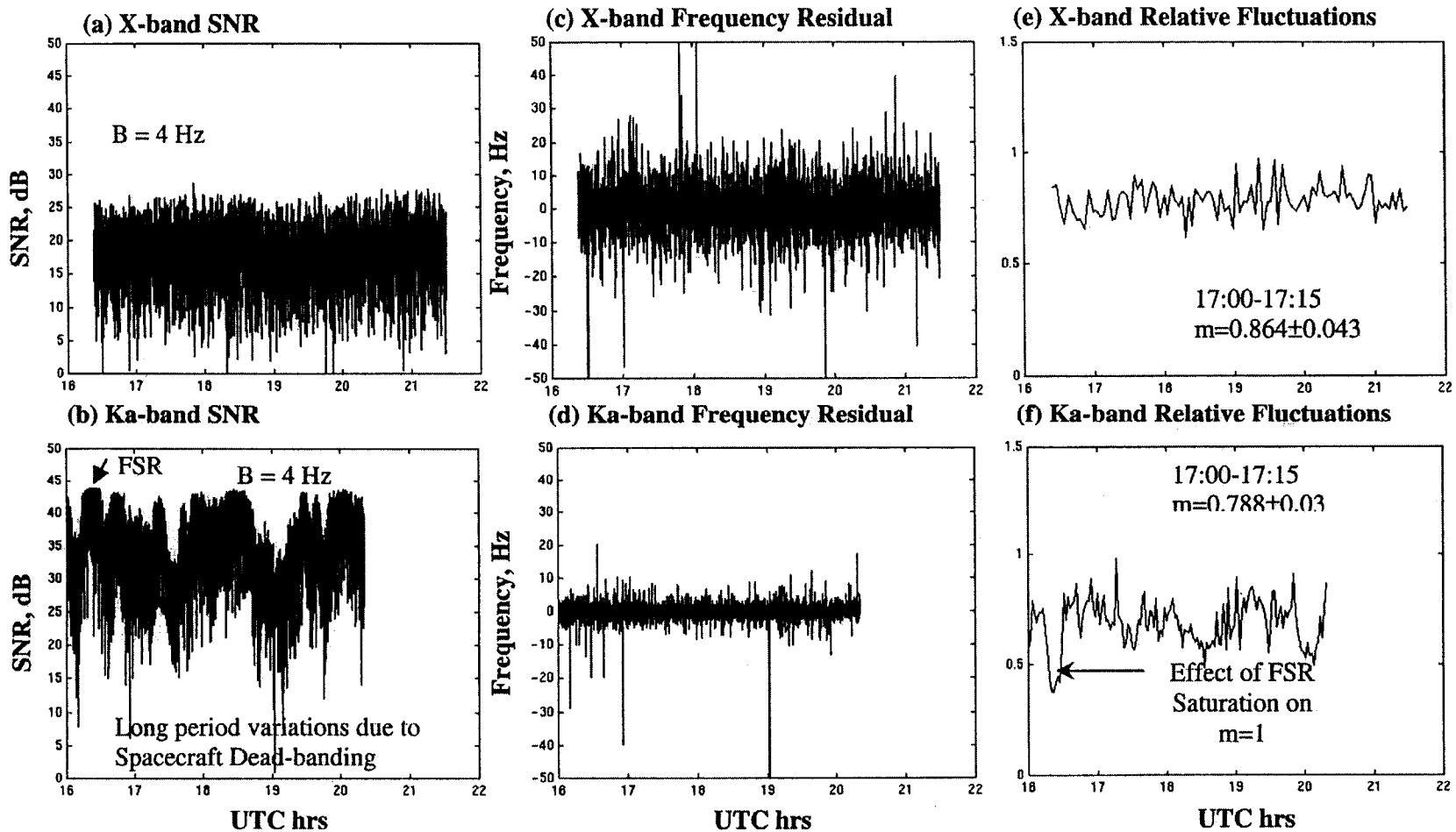


Figure 3. The first Cassini solar conjunction experimental results at X and Ka-bands. Data were recorded at DSS-13 on May 13 (134), 2000 for both X and Ka bands when the ray path has a minimum solar elongation angle ($SEP = 0.6^\circ$) or the closest distance from the Sun (2.4 solar radius). (a) X-band output SNR, (b) Ka-band output SNR, (c) X-band frequency residual, (d) Ka-band frequency residual, (e) X-band scintillation index, and (f) Ka-band scintillation index [9].

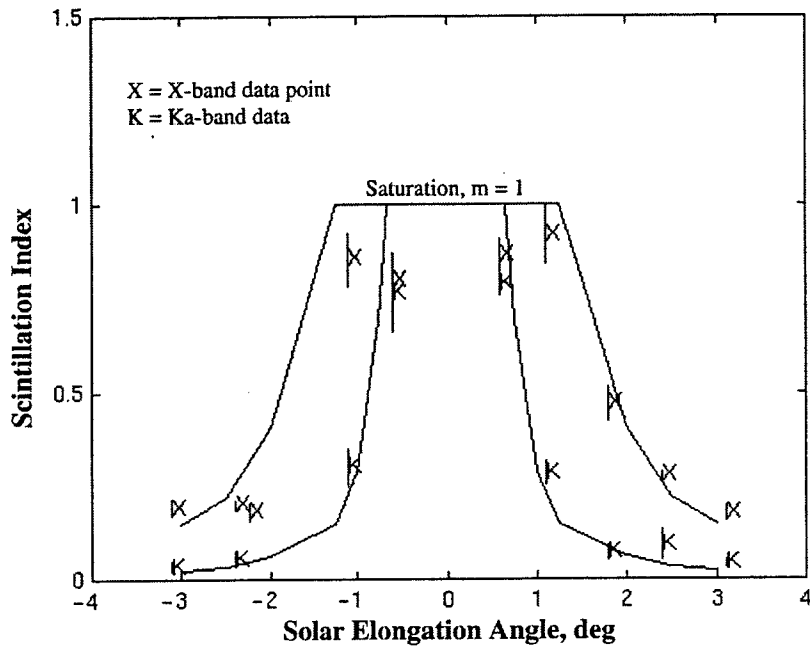


Figure 4. A plot of the observed scintillation indices from each of Cassini solar conjunction passes. The solid curves derived from previous measurements are also shown. Negative SEP angles denote ingress when positive for egress. The indicis are saturated at 1.0 [9].

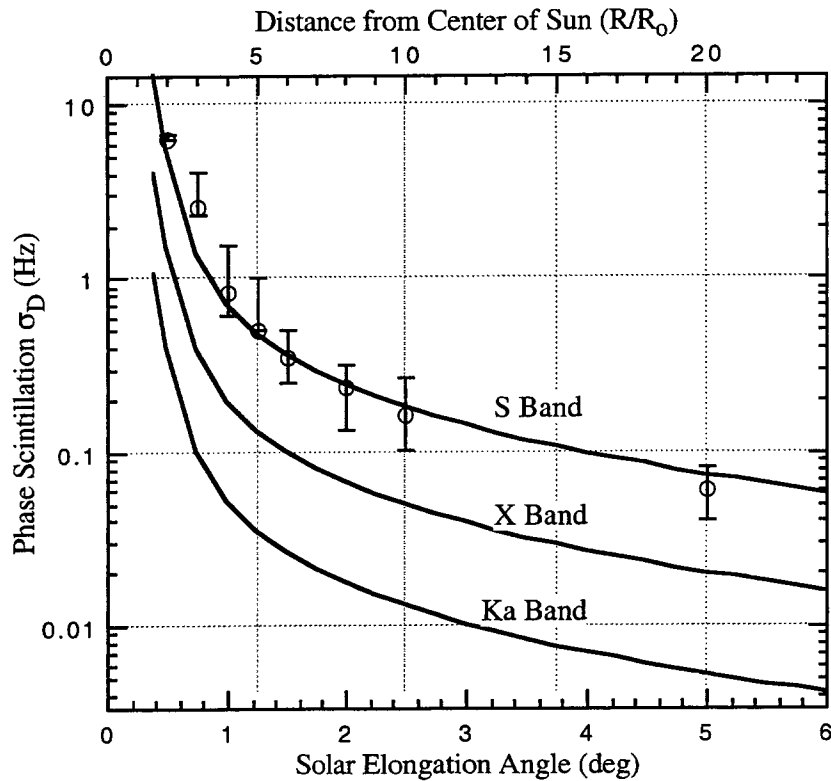


Figure 5. Phase scintillation (Doppler noise) dependence on solar elongation angles (or closest distance from Sun). Solid curves are plotted from Equation (5). Noted that there is no data available for both X and Ka bands.

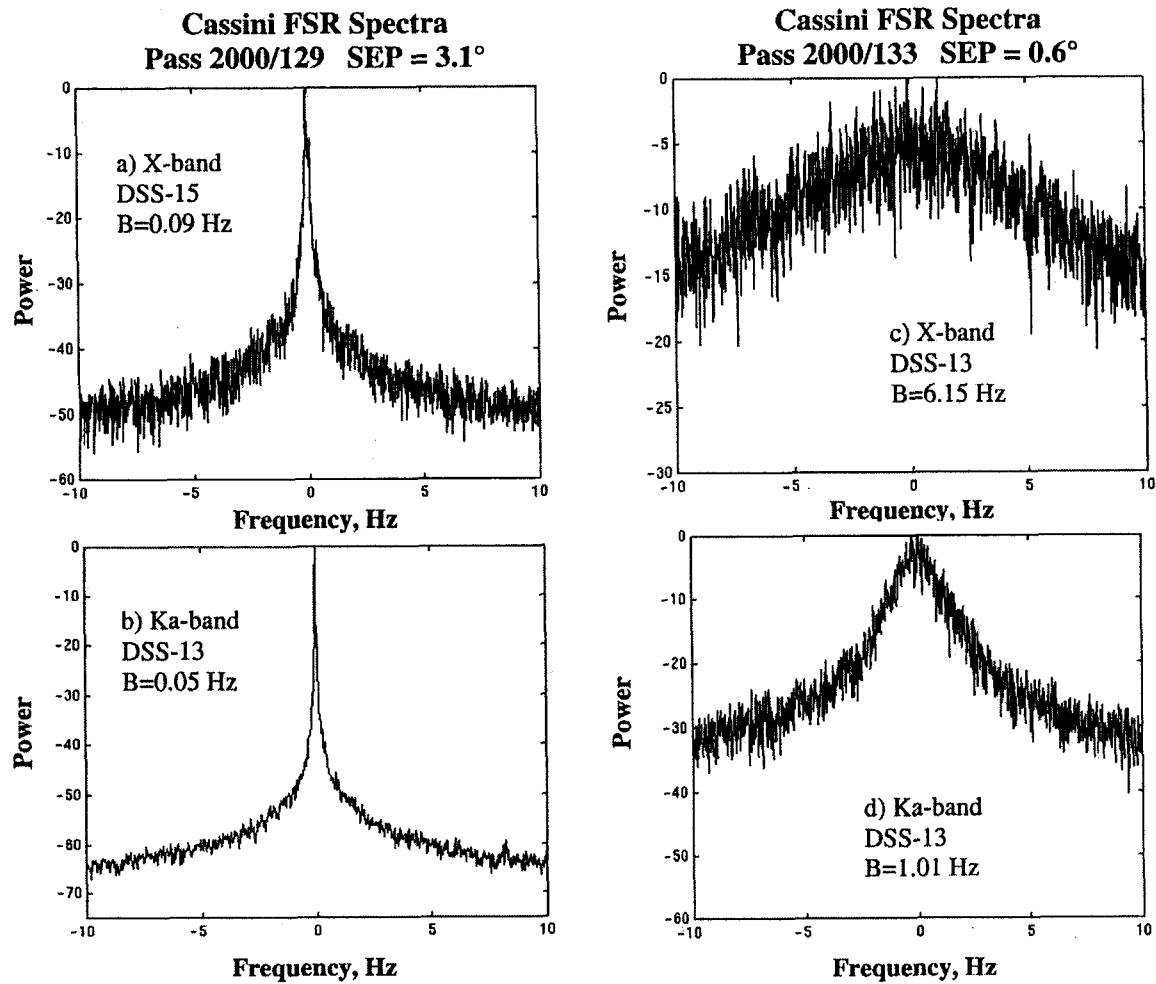


Figure 6. Radio signal spectral broadening bandwidth with decreasing solar elongation angle (or closest distance from Sun) for Cassini ray paths. Left panel shows a narrower bandwidth when SEP = 3.1° (12.4 R_{\odot}) for both (a) X-band and (b) Ka-band, while right panel shows a wider bandwidth when SEP = 0.6° (2.4 R_{\odot}) for both (c) X-band and (d) Ka-band [9].

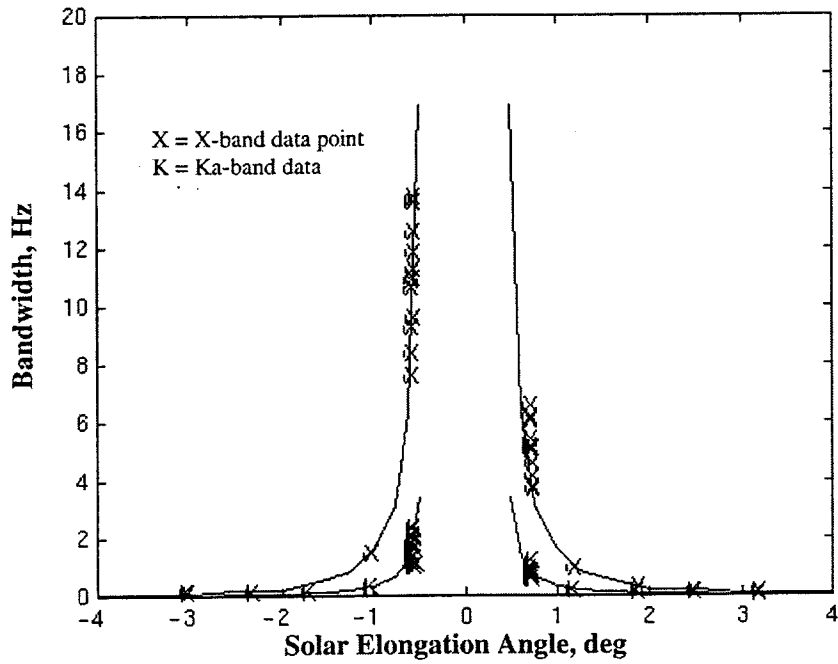


Figure 7. A plot of the observed spectral broadening versus SEP for each Cassini solar conjunction passes for representative 400-s periods during the quiet background. The solid curves are derived from an extrapolated model from S-band. Data are shown from ingress to egress [9].

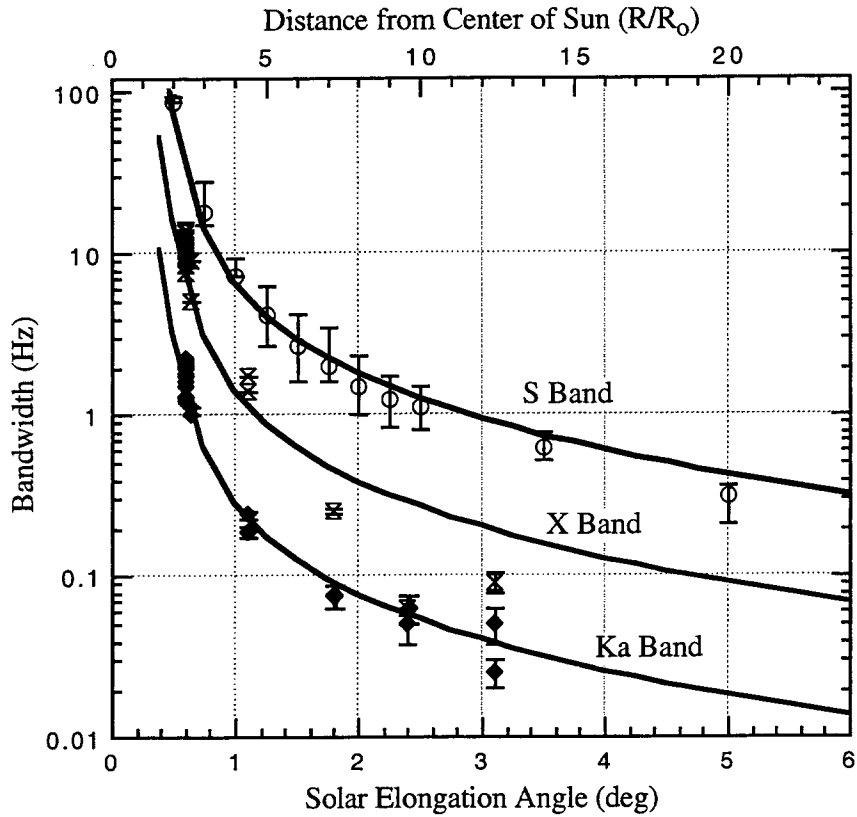


Figure 8. Spectral broadening dependence on solar elongation angle (or closest distance from Sun). Solid curves are plotted basing on Equation (11). both X and Ka band data are from Cassini experiment.